Supporting Information

Protein Apparent Dielectric Constant and its Temperature Dependence from Remote Chemical Shift Effects

Liaoyuan An[a], Yefei Wang[a], Ning Zhang[a], Shihai Yan[b], Ad Bax[c] and Lishan Yao[a]*

[a.] Laboratory of Biofuels, Qingdao Institute of Bioenergy and Bioprocess Technology, Chinese Academy of Sciences, Qingdao, 266061, China [b.] College of Chemistry and Pharmaceutical Sciences, Qingdao Agricultural University, Qingdao, 266109, China [c.] Laboratory of Chemical Physics, NIDDK, National Institutes of Health, Bethesda, MD, 20892-0520, USA

Methods and Material

Sample expression and purification. The 56-residue third IgG-binding domain of protein G, GB3, and the mutants K19A and K19E, were made by expression in Escherichia Coli BL21 (DE3*) cells, transformed with a pET-11 vector containing the GB3 or mutant gene. Details of the preparation and purification procedure have been described previously.[1] Mixed ^{15}N-labeled and ^{15}N/^{13}C-labeled protein samples were prepared, containing 20 mM sodium phosphate, 50 mM sodium chloride, pH 6.5, 5% D2O, in 550 μl volume. In the NaCl titration experiments, a small amount of concentrated NaCl solution (5 M) was added to the sample, which had been extensively dialyzed against distilled water to minimize the starting salt concentration, to reach NaCl concentrations of 0, 50, 100, 150 and 200 mM. Similarly, in the sodium phosphate titration experiments, a small amount of concentrated sodium phosphate (1 M, pH 6.5) was added to the sample, to reach final sodium phosphate concentrations of 1, 10, 20, 40, 60, 80 and 100 mM.

NMR spectroscopy. All NMR experiments were carried out on a Bruker Avance 600 MHz spectrometer, equipped with a z-axis gradient, triple resonance, cryogenic probe. 2D constant-time ^{15}N-^{1}H HSQC spectra were recorded using the sequence shown in Figure S1. Acquisition times were 63 (^{15}N) and 83 ms (^{1}H) with the data matrices consisting of 127*×1024* data points, where N* indicates N complex points. The spectra were recorded with 4 scans per FID. The measurements were also performed for the mixed sample (^{15}N-labeled K19A and ^{15}N/^{13}C-labeled WT, as well as ^{15}N labeled K19E and ^{15}N/^{13}C labeled WT, dissolved in a 10 mM sodium phosphate and pH 6.5 buffer) at 278, 288, 298, 308 and 313K to study the temperature effect on CSPs. The data were processed and analyzed using NMRPipe software.[2]

Molecular dynamics simulation. Molecular dynamics (MD) simulations were carried out with the program Gromacs 4.5,[3,4] using the Amber ff99SB force field[5] and TIP3P water. The starting coordinates were taken from the GB3 structure (pdb entry 2OED). The structures of the mutants were generated by tLeap of Amber 11.[6] All residues were assumed to be in their standard ionization states at pH 7.0. The protein was solvated by

adding 12.5Å TIP3P water in a rectangular box and Na^+ counter ions were used to neutralize the system. The Particle-Mesh-Ewald Method[7,8] was used to evaluate the contributions of the long-range electrostatic interactions. A non-bonded pair list cutoff of 10.0 Å was used and the non-bonded pair list was updated every 5 steps. All bonds to hydrogen atoms in the protein were constrained by using the LINC algorithm[9] whereas bonds and angles of water molecules were constrained by the SETTLE algorithm,[10] and a time step of 2 fs was used. The temperature was controlled by a modified Berendsen thermostat.[11] MD simulations (0.5 μs duration) were performed for WT, K19A and K19E GB3 mutants with the backbone heavy atoms restrained with a force constant of 10 kJ/Å^2 to their starting positions. Snapshots were saved every 200 ps. The electric field on each C^α atom was calculated by using Amber ff99SB charges for all atoms and averaged over 2500 MD snapshots, using no distance cut-off, and the field generated by the particles outside the box was neglected.

Quantum mechanical calculation. Quantum mechanical calculations were performed by using the Gaussian 09 program.[12] N-methylacetamide (NMA) was used as the model compound to study the electric field effect on the amide protein $^1H^N$ chemical shifts. The model was optimized at DFT/B3LYP[13] and MP2[14] with different basis sets (including Aug-cc-pvdz[15] to Aug-cc-pv6z for B3LYP, Aug-cc-pvdz and Aug-cc-pvtz for MP2) and then the chemical shifts were calculated with the GIAO[16] method in the presence or absence of an electric field of 0.001 au along the *x*, *y* or *z* axis, using the coordinate frame as defined in scheme 1. The shielding polarizability constant *A* was calculated using equation 1.

Dielectric constant fitting using CSPs. The values $\Delta\delta = (\Delta\delta_{K19E}/2 + \Delta\delta_{K19A})/2$ for 31 residues (excluding Q32) were used for fitting of the effective dielectric constant. The CSPs in the high salt buffer (20 mM sodium phosphate, 50 mM sodium chloride) were linearly fitted to those measured in water (Figure S2) which yielded a slope of 1.62. The Δδ values (in the high salt buffer) were scaled up by multiplying by 1.62 and averaged with Δδs from the water, which were then used for the dielectric constant fitting. The gas phase electric field along the vector *A*, at each CSP site, was calculated by using Coulumb's law with partial charges assigned to Nζ, Hζ1, Hζ2, Hζ3 and Cε atoms of

residue K19 (Table S3). The PDB structure 2OED[17] was used for the calculation. Eq. 3 was used to predict the $\Delta\delta$ values which were fitted to the experimental values by systematically changing the dielectric constant ε_a.

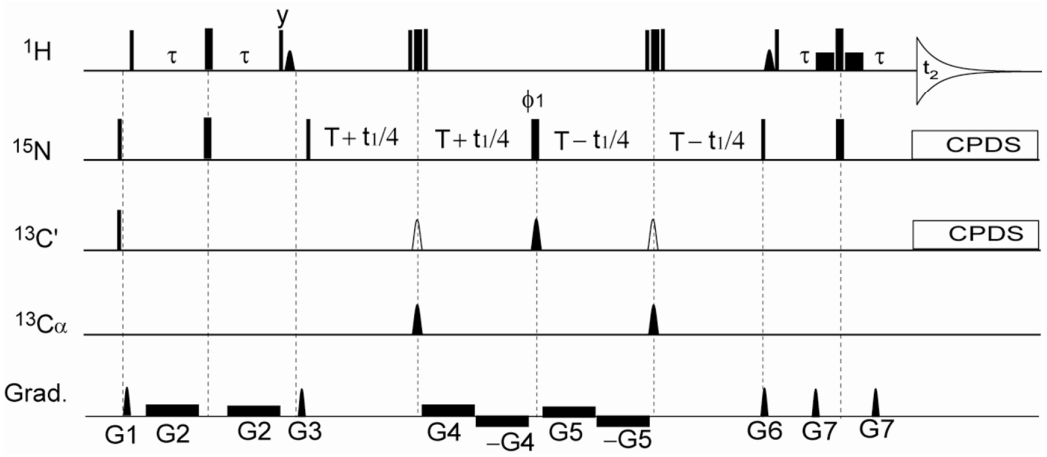

Figure S1. Pulse sequence used to measure the ^{15}N-^{1}H chemical shift of the mixed ^{15}N/^{13}C and ^{15}N labeled sample. Narrow and wide pulses correspond to 90º and 180º flip angles, respectively. All the ^{1}H pulses are centered on the H_2O resonance. The ^{13}C'/C$^{\alpha/\beta}$ nuclei are decoupled by 800 μs hyperbolic secant shaped pulses,[18] centered at 176.6 and 56.6 ppm respectively. Composite pulses (90_x-180_y-90_x) are applied to decouple the ^{1}H nucleus during ^{15}N evolution. The shaped ^{1}H pulses (center lobe of sinc function, 1 ms duration) correspond to a flip angle of 90º to selectively rotate the water magnetization. The WATERGATE method[19] was used to suppress the water signal, with two 1-ms rectangular pulses before and after the last ^{1}H 180º hard pulse. Delays: τ= 2.6 ms (incl. duration of weak ^{1}H pulse), T = 16.6 ms. The phases of all pulses are *x* unless indicated. Phase cycling: ϕ_1 = x, y, -x, -y; Rec. = x, -x. The empty shaped ^{13}C' pulses are omitted for generating the spectrum of ^{15}N labeled sample minus that of the ^{15}N/^{13}C labeled sample, and are applied but with the solid shaped ^{13}C' pulse omitted for generating the sum of the two spectra. Pulsed field gradients $G_{1,3,6,7}$ are sine-bell shaped with maximum gradient strengths at their midpoints of 10.2 G/cm, 4.2 G/cm, 28.2 G/cm, and 18.6 G/cm respectively. G_2, G_4 and G_5 are rectangular pulses with a strength of 0.6 G/cm, and serve to prevent radiation damping of the water signal. The durations for gradient pulses are $G_{1,2,3,4,5,6,7}$ = 1.5, 2.6, 1.3, T/2+t_1/8, T/2–t_1/8, 1.3, 1.5, 1.5 ms. All gradient pulses are applied along the z axis.

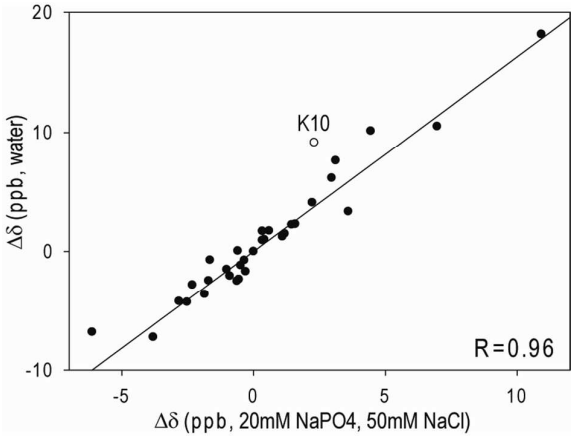

Figure S2. Correlation of $\Delta\delta$ CSP values at the buffer 20mM sodium phosphate and 50mM NaCl versus at water. The best fitted solid line is $y = 1.62x$.

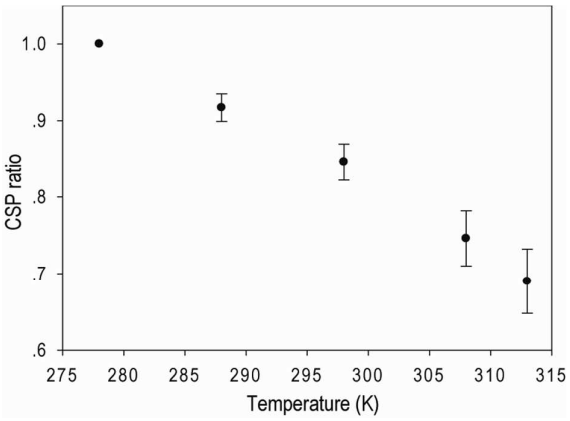

Figure S3. Slope of the best-fit linear correlation between CSP values measured for $\Delta\delta_{K19A}$ at different temperatures against values measured at 278 K.

Table S1. Amide ^{1}H chemical shift differences, ΔδK19A and ΔδK19E, and the WT ^{13}C isotope shift corrections as observed for $^{1}H^{N}$ in WT GB3 at 298K. Distance of amide nitrogen of each residue to the Cg atom of K19 is also listed based on the structure 2OED.[17]

Residue	Distance to K19 Cγ	$\Delta\delta_{K19E}{}^{a}$ (ppb)	$\Delta\delta_{K19E}{}^{b}$ (ppb)	$\Delta\delta_{K19A}{}^{a}$ (ppb)	$\Delta\delta_{K19A}{}^{b}$ (ppb)	$^{13}C^{a}$ Isotope shift (ppb)
Y3	6.3	-9.0	-27.1	-36.9	-46.7	-1.1
K4	9.1	10.3	28.3	3.9	6.3	-0.9
L5	11.1	-2.1	-7.5	1.3	1.8	-0.5
V6	14.5	4.0	9.4	-2.8	-2.8	-0.5
I7	16.9	-5.0	-9.8	-2.2	-2.0	-0.9
N8	20.2	-1.1	2.2	-2.2	-0.6	-1.0
G9	22.3	1.9	8.6	-0.5	1.9	-1.6
K10	25.4	3.6	26.5	0.3	10.4	-1.7
T11	25.8	-0.2	5.2	-1.3	1.8	-1.4
L12	23.4	-3.5	-3.8	-2.3	-1.9	-1.3
K13	21.2	2.3	8.6	-0.4	2.0	-1.6
G14	18.8	5.8	17.5	-0.1	2.9	-1.1
E15	15.5	13.0	N/A	2.8	N/A	-2.2
T16	12.0	1.1	8.3	-2.9	0.1	-0.8
T17	8.4	27.6	54.5	11.6	14.2	-1.5
T18	5.5	-25.0	-47.1	3.4	3.0	-0.6
K19	2.8	62.0	104.3	-39.4	-36.8	-1.6
A20	4.8	-222.8	-384.2	3.0	N/A	-0.7
V21	8.0	23.7	73.6	6.9	23.2	-1.4
D22	10.2	1.5	5.8	-4.5	-3.4	-1.5
A23	12.0	2.8	0.8	-5.2	-6.2	-1.5
E24	13.5	17.3	58.1	2.7	13.0	-1.8
T25	12.3	N/A	N/A	N/A	N/A	N/A
A26	10.1	-14.3	-20.4	1.7	6.2	-1.9
E27	11.9	N/A	N/A	N/A	N/A	N/A
K28	13.4	-3.3	-8.4	-4.0	-4.7	-1.3
A29	11.9	-8.5	-6.8	-7.3	-2.4	-2.0
F30	11.7	-11.7	-13.8	-14.5	-10.7	-1.1
K31	14.5	-6.1	-12.1	1.8	1.0	-1.4
Q32	15.4	8.0	14.1	1.2	2.4	-1.3
Y33	14.6	-12.0	-20.3	-9.1	-7.5	-1.9
A34	16.0	-9.2	-15.0	-2.0	-1.2	-1.3
N35	18.6	14.6	27.4	3.9	2.1	-0.9
D36	18.9	-2.3	0.5	-4.2	-1.6	-1.3
N37	19.2	-3.2	-4.0	-2.3	-1.2	-1.9
G38	21.5	1.4	7.6	-1.6	1.2	-1.4
V39	21.7	-3.5	-8.1	-2.0	-2.6	-1.7
D40	23.2	-8.1	-17.8	-3.5	-3.1	-1.3
G41	23.3	0.8	5.6	-0.3	1.3	-1.5
V42	23.6	-1.7	2.5	-1.7	1.2	-2.2
W43	21.8	-2.5	-2.2	-1.3	-0.8	-1.2
T44	19.9	-3.3	-9.0	-3.9	-5.9	-0.3
Y45	18.6	1.0	4.6	-0.7	1.1	-1.6
D46	17.3	-5.3	-7.1	-2.6	-1.3	-2.0
D47	17.4	10.1	37.2	2.1	9.1	-1.1

A48	17.5	5.7	25.9	1.6	7.5	-1.2
T49	16.1	4.2	20.1	0.5	6.3	-2.3
K50	13.7	11.8	34.6	5.2	10.7	-1.9
T51	13.3	17.8	55.4	9.9	19.7	-2.0
F52	13.8	-18.7	-37.9	-1.7	-3.1	-0.5
T53	16.7	2.1	6.3	-0.9	0.0	-0.4
V54	18.5	-9.0	-23.5	-4.4	-7.4	-0.9
T55	21.7	-4.0	-6.6	-1.7	-2.2	-1.3
E56	24.4	-2.8	-7.5	-1.7	-2.4	-1.3

[a.] The sample is in 20 mM sodium phosphate, 50 mM sodium chloride, 5% D_2O, pH 6.5 buffer.

[b.] The sample is in distilled water, 5% D_2O.

Table S2. Amide ^1H shielding polarizability constants (in units of ppm-Å^2/e) from quantum mechanical DFT and MP2 calculations of NMA

Basis set	A_x	A_y	A_z	$\|A\|^a$	θ(°)^b
DFT/B3LYP					
	18.8	–6.8	–0.2	20.0	19.9
Aug-cc-pvtz	18.9	–6.6	–0.2	20.0	19.2
	18.9	–6.6	–0.2	20.0	19.2
	19.0	–6.6	–0.2	20.0	19.3
	19.0	–6.7	–0.2	20.1	19.3
MP2					
Aug-cc-pvdz	19.6	–7.1	–0.3	20.8	19.9
Aug-cc-pvtz	19.8	–6.9	–0.2	21.0	19.2

[a.] $|A|$ is defined as $(A_x^2 + A_y^2)^{0.5}$. The contribution from A_z, which is small, is neglected.

[b.] θ is the angle between the vector A and the N–H bond. Definition of the coordinate system is shown in Scheme 1.

Table S3. Partial charges for the side chain of K19.

Nζ	-0.32e
Hζ1	0.33e
Hζ2	0.33e
Hζ3	0.33e
Cε	0.33e

References

(1) Yao, L.; Ying, J.; Bax, A. *J. Biomol. NMR* **2009**, *43*, 161.

(2) Delaglio, F.; Grzesiek, S.; Vuister, G. W.; Zhu, G.; Pfeifer, J.; Bax, A. *J. Biomol. NMR* **1995**, *6*, 277.

(3) Hess, B.; Kutzner, C.; van der Spoel, D.; Lindahl, E. *J. Chem. Theory Comput.* **2008**, *4*, 435.

(4) Van der Spoel, D.; Lindahl, E.; Hess, B.; Groenhof, G.; Mark, A. E.; Berendsen, H. J. C. *J. Comput. Chem.* **2005**, *26*, 1701.

(5) Hornak, V.; Abel, R.; Okur, A.; Strockbine, B.; Roitberg, A.; Simmerling, C. *Proteins* **2006**, *65*, 712.

(6) Case, D. D., TA; Cheatham, TE; Simmerling, CL; Wang, J; Duke, RE; Luo, R; Walker, RC; Zhang, W; Merz, KM; Roberts, B; Wang, B; Hayik, S; Roitberg, A; Seabra, G; Kolossvary, I; Wong, KF; Paesani, F; Vanicek, J; Liu, J; Wu, X; Brozell, SR; Steinbrecker, T; Gohlke, H; Cai, Q; Ye, X; Wang, J; Hsieh, M-J; Cui, G; Roe, DR; Mathews, DH; Seetin, MG; Sagui, C; Babin, V; Luchko, T; Gusarov, S; Kovalenko, A; Kollman, PA, **2010**, AMBER 11, University of California, San Francisco.

(7) Darden, T.; York, D.; Pedersen, L. *J. Chem. Phys.* **1993**, *98*, 10089.

(8) Essmann, U.; Perera, L.; Berkowitz, M. L.; Darden, T.; Lee, H.; Pedersen, L. G. *J. Chem. Phys.* **1995**, *103*, 8577.

(9) Hess, B.; Bekker, H.; Berendsen, H. J. C.; Fraaije, J. G. E. M. *J. Comput. Chem.* **1997**, *18*, 1463.

(10) Miyamoto, S.; Kollman, P. A. *J. Comput. Chem.* **1992**, *13*, 952.

(11) Berendsen, H. J. C. *Nato Adv Sci I E-App* **1991**, *205*, 139.

(12) Frisch, M. J. T., G. W.; Schlegel, H. B.; Scuseria, G. E. Robb, M. A.; Cheeseman, J. R.; Scalmani, G.; Barone, V.; Mennucci, B.; Petersson, G. A.; Nakatsuji, H.; Caricato, M.; Li, X.; Hratchian, H. P.; Izmaylov, A. F.; Bloino, J.; Zheng, G.; Sonnenberg, J. L.; Hada, M.; Ehara, M.; Toyota, K.; Fukuda, R.; Hasegawa, J.; Ishida, M.; Nakajima, T.; Honda, Y.; Kitao, O.; Nakai, H.; Vreven, T.; Montgomery, J. A.; Peralta, Jr., J. E.; Ogliaro, F.; Bearpark, M.; Heyd, J. J.; Brothers, E.; Kudin, K. N.; Staroverov, V. N.; Keith, T.; Kobayashi, R.; Normand, J.; Raghavachari, K.; Rendell, A.; Burant, J. C.; Iyengar, S. S.; Tomasi, J.; Cossi, M.; Rega, N.; Millam, J. M.; Klene, M.; Knox, J. E.; Cross, J. B.; Bakken, V.; Adamo, C.; Jaramillo, J.; Gomperts, R.; Stratmann, R. E.; Yazyev, O.; Austin, A. J.; Cammi, R.; Pomelli, C.; Ochterski, J. W.; Martin, R. L.; Morokuma, K.; Zakrzewski, V. G.; Voth, G. A.; Salvador, P.; Dannenberg, J. J.; Dapprich, S.; Daniels, A. D.; Farkas, O.; Foresman, J. B.; Ortiz, J. V.; Cioslowski, J.; Fox, D. J.; Gaussian 09, Revision B.01 ed.; Gaussian, Inc.: Wallingford CT: 2010.

(13) Becke, A. D. *J. Chem. Phys.* **1993**, *98*, 5648.

(14) Headgordon, M.; Pople, J. A.; Frisch, M. J. *Chem Phys Lett* **1988**, *153*, 503.

(15) Papajak, E.; Zheng, J. J.; Xu, X. F.; Leverentz, H. R.; Truhlar, D. G. *J. Chem. Theory Comput.* **2011**, *7*, 3027.

(16) Ruud, K.; Helgaker, T.; Bak, K. L.; Jorgensen, P.; Jensen, H. J. A. *J. Chem. Phys.* **1993**, *99*, 3847.

(17) Ulmer, T. S.; Ramirez, B. E.; Delaglio, F.; Bax, A. *J. Am. Chem. Soc.* **2003**, *125*, 9179.

(18) Silver, M. S.; Joseph, R. I.; Hoult, D. I. *J. of Magn. Reson.* **1984**, *59*, 347.

(19) Sklenar, V.; Piotto, M.; Leppik, R.; Saudek, V. *J. of Magn. Reson. A* **1993**, *102*, 241.